A Statistical Analysis of the Relationship between Upper-Tropospheric Cold Low and Tropical Cyclone Track and Intensity Change over the Western North Pacific

NA WEI

State Key Laboratory of Severe Weather, Chinese Academy of Meteorological Sciences, and University of Chinese Academy of Sciences, Beijing, China

YING LI

State Key Laboratory of Severe Weather, Chinese Academy of Meteorological Sciences, Beijing, China

DA-LIN ZHANG

State Key Laboratory of Severe Weather, Chinese Academy of Meteorological Sciences, Beijing, China, and Department of Atmospheric and Oceanic Science, University of Maryland, College Park, College Park, Maryland

ZI MAI AND SHI-QI YANG

State Key Laboratory of Severe Weather, Chinese Academy of Meteorological Sciences, Beijing, China

(Manuscript received 20 October 2015, in final form 20 January 2016)

ABSTRACT

The geographical and temporal characteristics of upper-tropospheric cold low (UTCL) and their relationship to tropical cyclone (TC) track and intensity change over the western North Pacific (WNP) during 2000–12 are examined using the TC best track and global meteorological reanalysis data. An analysis of the two datasets shows that 73% of 346 TCs coexist with 345 UTCLs, and 21% of the latter coexist with TCs within an initial cutoff distance of 15°. By selecting those coexisted systems within this distance, the possible influences of UTCL on TC track and intensity change are found, depending on their relative distance and on the sectors of UTCLs where TCs are located. Results show that the impact of UTCLs on TC directional changes are statistically insignificant when averaged within the 15° radius. However, left-turning TCs within 5° distance from the UTCL center exhibit large deviated directional changes from the WNP climatology, due to the presence of highly frequent abrupt left turnings in the eastern semicircle of UTCL. The abrupt turnings of TCs are often accompanied by their slow-down movements. Results also show that TCs seem more (less) prone to intensify at early (late) development stages when interacting with UTCLs compared to the WNP climatology. Intensifying (weakening) TCs are more distributed in the southern (northern) sectors of UTCLs, with less hostile conditions for weakening within 9°–13° radial range. In addition, rapid intensifying TCs take place in the south-southwest and east-southeast sectors of UTCLs, whereas rapid weakening cases appear in the western semicircle of UTCLs due to their frequent proximity to mainland coastal regions.

1. Introduction

The upper-tropospheric cold low (UTCL) is one of the closed cyclonic circulation systems that occur frequently over the tropical and subtropical western North Pacific (WNP), which is also the active region for the development of tropical cyclones (TCs). Clearly, some UTCLs and TCs are doomed to meet and affect each other inevitably during the typhoon season (Riehl 1948). In general, most UTCLs are generated out of the tropical upper-tropospheric (UT) trough (TUTT; Palmer 1953; Sadler 1976) after forming a low pressure center (often referred to as the TUTT cell), some others are related to cutoff lows in the midlatitude westerlies (Palmén 1949; Molinari and Vollaro 1989; Postel and Hitchman 1999).

A number of observational studies (e.g., Xu and Wang 1979; Chen et al. 1988; Chen and Chou 1994) have

Corresponding author address: Dr. Ying Li, State Key Laboratory of Severe Weather, Chinese Academy of Meteorological Sciences, No. 46, Zhongguancun St., Beijing 100081, China.
E-mail: liying@camscma.cn

DOI: 10.1175/MWR-D-15-0370.1

examined the characteristics of UTCLs over WNP, and noted that on average there were about 2.5 UTCLs per day appearing near 23°N during the warm season and the maximum UTCL frequency occurs in August. Most of them moved westward at a mean speed of 4.1 m s^{-1} (or 14.8 km h^{-1}). The average life span of UTCLs is about 6.3 days, which is close to that of TCs. Kelly and Mock (1982) used four summers of rawinsonde data to form a three-dimensional composite of 117 UTCLs, showing that the composite low is confined to the 700–100-hPa layer with an approximate radius of 800 km. The composite maximum circulation occurs at 200 hPa while the associated cold anomaly is peaked at 300 hPa. The northwest portion of the cold low is characterized by subsidence with minimum cloudiness, whereas the southeast portion is dominated by ascent with maximum cloudiness. These characteristics are generally in good agreement with the observations of UTCLs over the Atlantic (Carlson 1967; Miller and Carlson 1970; Erickson 1971), and they have also been confirmed by satellite data over the WNP region (Chen et al. 1988).

Previous studies indicated that UTCLs could produce favorable influences on the development of TCs (e.g., Chen and Ding 1979; Xu and Wang 1979). Sadler (1976) summarized the following two positive effects of UTCLs on TC development: decreasing vertical wind shear (VWS) on the southern side of UTCLs, and increasing UT mass evacuation due to the presence of divergent outflow on the southern and eastern sides of UTCLs. Later, Sadler (1978) further verified the importance of vigorous outflows associated with UTCLs in determining TC genesis in proximity to a UTCL, which tends to take place under the diffluent anticyclonically curved outflow to the east of a UTCL. Chen and Chou (1994) found that 87% of UTCLs contain ''jet streaks'' (20–30 m s^{-1}) with UT asymmetrical cloud structures in the outer regions. Because of the presence of weak inertial stability, the existence of such jet streaks tends to enhance the UT divergence on the anticyclonic shear side, thereby favoring the intensification of TCs (Shi et al. 1990; Rappin et al. 2011; Sears and Velden 2014), especially the genesis of TCs. This type of TC genesis was studied by Kelly and Mock (1982), who hypothesized that the UT divergence and ascending motion associated with a UTCL may help inducing low-level mass and moisture convergence that facilitate the generation of deep convection and the ''bottom-up'' growth of cyclonic vorticity favoring TC genesis (Zhang and Bao 1996a,b; Hendricks et al. 2004; Montgomery et al. 2006). The enhanced UT divergence in the weak inertial stability regions appears to facilitate the lower-level lifting and convective development in the core region (Sears and Velden 2014), sometimes leading to the formation of TC. Previous studies also indicated that the increased convergence of eddy angular momentum resulting from the interaction of TCs with upper-level disturbances may facilitate TC intensification (e.g., Molinari and Vollaro 1989; Davidson and Kumar 1990; DeMaria et al. 1993; Hanley et al. 2001; Hanley 2002). Cyclonic potential vorticity (PV) advection toward the TC core during such events has also been demonstrated to play a role in TC intensification (e.g., Molinari et al. 1995, 1998; Montgomery and Farrell 1993; Leroux et al. 2013).

In addition, some rapid intensification (RI) phenomena are found to be related to UTCLs. DeMaria et al. (1993) found that a sizeable number of TCs with RI experience a period of enhanced eddy flux convergence of angular momentum aloft due to their interactions with UTCLs at lower latitudes or UT troughs in the midlatitudes. The RI of Hurricane Opal (1995) was argued to be initiated by its interaction with a trough, which enhanced convective activity in the inner core (Bosart et al. 2000). Li et al. (2012) noted that the RI of Typhoon Meranti (2010) offshore was closely related to the passage of a UTCL nearby. Leroux et al. (2013) found that the PV anomaly associated with a cutoff low descended to midlevel circulations, leading to the RI of Hurricane Dora (2007). Shieh et al. (2013) also found significant influences of a traveling UT ''inverted'' trough on the RI of Typhoon Vicente (2012).

Despite many studies on the positive influences of UTCLs, some studies have argued that the UT troughs play a minimal role in deepening TCs (e.g., Persing et al. 2002) and that they may even weaken TCs as asymmetric UT circulation often induces intense VWS, the so-called ''unfavorable troughs.'' In Hanley et al.'s (2001) composite study, such unfavorable interaction was attributed to a PV maximum of strong intensity and/or horizontal extent exceeding that of the TC inducing larger VWS over the TC center. Molinari et al. (1998) discussed the importance of scale reduction of a positive PV anomaly in TC intensity changes prior to their superposition. Fitzpatrick et al. (1995) examined the VWS variation on the prediction of TC genesis and intensity change under the influence of a TUTT. They speculated that the TC intensity change forecasts would be improved if the VWS errors resulting from erroneous estimation (e.g., unrealistic weakening) of a TUTT and associated cold lows over the Caribbean Sea could be eliminated.

The UTCL has also been considered as an important factor in influencing TC track changes, which could be achieved by modifying larger-scale steering flows. Chen and Ding (1979) indicated the presence of an interaction between a UTCL and a typhoon that is similar to that of binary typhoon vortices (e.g., Hart and Evans 1999).

That is, the UTCL could alter the environmental flow around the typhoon. Chen et al. (2002) simulated the steering effect of a UTCL when a TC enters its peripheral, and the attracting effect when a TC gets close enough to a UTCL. The steering effect mainly depends on the relative orientation of the two systems. For example, if a TC is located on the southwest of a UTCL, northward winds on the west of the UTCL could lead to the TC's stagnation or southward movement. Of course, the quantitative effects on TC track may differ, depending on the intensity, distance, and size of the UTCL. Fei and Fan (1992, 1993) performed an idealized modeling study of the impact of UTCLs on typhoon movement, showing that the distribution of the UT divergence has significant influences on typhoon motion within their interaction radius of about 9° (latitude–longitude). To provide operational guidance for TC forecasters, Patla et al. (2009) developed the first conceptual model of TC track prediction regarding the TC–TUTT cell interaction based on the interaction radius of 1700 km (~15° latitude–longitude). The likelihood of TC movement, including moving direction and speed, near a UTCL was discussed [see Fig. 20 in Patla et al. (2009)]. Moreover, Typhoons Meranti (2010) and Vicente (2012) were observed to alter their movement directions abruptly during their interaction with UT asymmetric flows (Li et al. 2012; Shieh et al. 2013).

It is evident from the above review that the previous studies have indicated both the positive and negative effects of UTCLs on TC development. However, it is unclear under what configuration a UTCL would exert positive or negative impact on a nearby TC. A statistical study with a large sample size appears to be highly desirable to help gain insight into the relationship between the two types of vortices. Thus, the objectives of this study are to (i) examine the geographical and temporal distributions of UTCLs in relation to TCs occurring over WNP; (ii) investigate the statistical characteristics of TCs interacting with UTCLs; and (iii) explore statistically the relationship between TC track and intensity change and UTCL, in an attempt to help improve our understanding and prediction of the influences of UTCL on TC track and intensity change. The above objectives will be achieved by analyzing the WNP best track and global reanalysis data during the recent 13-yr (i.e., 2000–12) period.

The next section provides a description of the datasets and methodology employed in the present study. Section 3 examines the statistical characteristics of UTCLs and TCs in the WNP, including their geographical and temporal distributions. Section 4 presents a statistical analysis of the possible influences of UTCL on TC track and intensity change, including the probability of TC abrupt turnings and rapid intensity changes. A summary and conclusions are given in the final section.

2. Data and methodology

In this study, the Shanghai Typhoon Institute of the China Meteorological Administration (CMA/STI) best track data from 2000 to 2012 (http://tcdata.typhoon.gov.cn/en/zjljsjj_zlhq.html) are used to describe TC track and intensity, including central positions in latitude and longitude, and maximum sustained surface wind speeds (V_{MAX}) at 6-hourly intervals along TC trajectories. Note that V_{MAX} was recorded as integers (Ying et al. 2014), and most frequently, as a multiple of 5 m s^{-1}. As will be shown in section 4b, this will cause uncertainties in estimating intensity changes of some TCs that are smaller than the 5 m s^{-1} discretization interval. The TC intensities are classified into six categories, depending on their 2-min mean V_{MAX}: tropical depression (TD; 10–17 m s^{-1}), tropical storm (TS; 18–24 m s^{-1}), severe tropical storm (STS; 25–33 m s^{-1}), typhoon (TY; 34–41 m s^{-1}), severe typhoon (STY; 42–51 m s^{-1}), and supertyphoon (Super TY; stronger than 51 m s^{-1}).

UTCLs are identified by using upper-air weather maps at 6-hourly intervals over the tropical and subtropical areas of WNP (i.e., over the "target" domain of 0°–35°N, 100°E–180° during all TCs' life spans). A cold low is defined as a closed depression with a cold air center in the upper troposphere. The National Centers for Environmental Prediction Final Operational Global Analysis (NCEP FNL; 1° × 1°, 6-hourly, http://rda.ucar.edu/datasets/ds083.2) datasets are chosen to provide the geopotential height and horizontal wind fields at 200 hPa and temperature at 300 hPa. The two levels are used to analyze UTCLs mainly because the most obvious cyclonic circulation occurs at 200 hPa and the strongest cold anomaly is usually found at 300 hPa (Kelly and Mock 1982). Thus, a UTCL event is assumed to begin when a closed geopotential height contour at 10-gpm intervals and a cyclonic circulation both appear at 200 hPa, together with a cold center at 300 hPa (i.e., a minimum in temperature at 1-K intervals). This event may be discontinuous as the closed contour may disappear temporarily. If so, that moment is considered as a time without the UTCL event. The termination timing of a UTCL event is determined when the closed height contour disappears permanently. The UTCL centers are evaluated by identifying the minimum wind speed in the cyclonic circulation (with the position errors of less than ±1° latitude–longitude) at 200 hPa. Only those UTCLs that sustained for at least 1 day are considered. A UTCL "best track" dataset is then created to match TC's during the TC's life span.

Note that some UTCLs could be transformed to TCs or induce TC genesis. For example, Davis and Bosart (2004) indicated that nearly half of the Atlantic TCs during the years of 2000–03 were formed from extratropical disturbances, some out of cutoff lows, the so-called tropical transition. The formation of TCs from UTCLs is not included in this statistical analysis, but their coexistence and subsequent interaction with UTCLs are included. Thus, UTCLs in our study only refer to those coexisting with TCs.

A midlatitude cutoff low is identified when a cutoff low from the midlatitudes moves to the WNP without merging with a TUTT. Otherwise, UTCLs associated with TUTTs are referred to as TUTT cells. Then, the number of different types of UTCLs and the times of their appearances can be identified, respectively. Note that by definition the appearance of a UTCL is counted once when a UTCL coexisting with a TC, and twice if the same UTCL coexisting with two TCs. We hereafter call "TCs coexisting with UTCLs" as TCs that coexist with UTCLs in the analyzed domain. Also, a frequency is defined as the times of events (at 6-h intervals) associated with TCs or UTCLs during the 13-yr period, and an event every 6 h as one case.

Interaction between a UTCL and a TC is hard to define, as the true interaction radius varies from case to case, depending on the intensity and size of the TC and UTCL as well as their relative distance and orientation. In fact, it is one of the objectives of this study to examine statistically through the student significance t test at what distance the UTCL–TC interaction would become significant. For the sake of statistical analysis, here we simply use the 15° latitude–longitude as the cutoff radius for vortex–vortex interaction, following Patla et al. (2009) who used an interaction radius of 1700 km to trace the influence of TUTT cells. This 15° distance also appears to be reasonable, based on the potential vorticity inversion of either baroclinic waves (Huo et al. 1999) or a hurricane (Kieu and Zhang 2010). As will be shown later, the selected 15° interaction distance affects little the quantitative results of this study after examining the directional and intensity changes of TCs as a function of distance from UTCLs. On the other hand, from a statistical sense, the results so obtained will help to reveal to what extent TC development is influenced by UTCLs and how the two systems are correlated within the 15° interaction distance.

3. Statistical characteristics

During the years of 2000–12, a total of 346 TCs occurred over WNP, and 251 (~73%) TCs were found to coexist with UTCL activity in the target domain

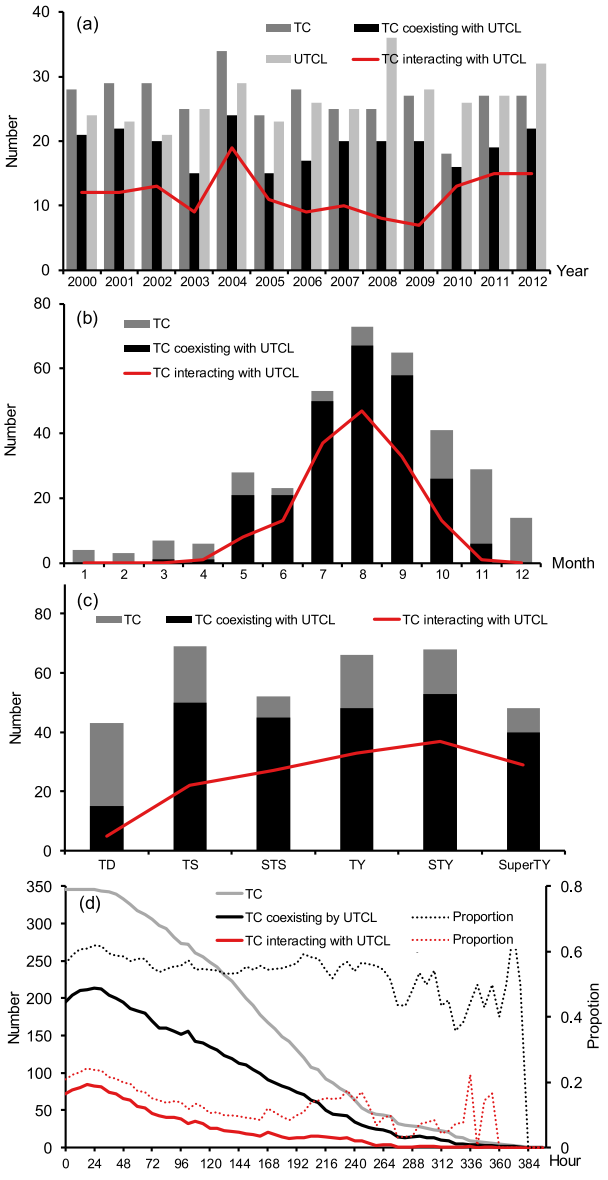

FIG. 1. The numbers of all TCs and UTCLs, TCs coexisting with UTCLs, and TCs interacting with UTCLs over WNP during the period of 2000–12, which are classified by (a) year, (b) month, (c) maximum TC intensity categories reached during their life spans, and (d) TC life spans (hours after reaching TD). Black (red) dotted lines in (d) denote the proportion of the number of TCs coexisting with (interacting with) UTCLs with respect to the total WNP TCs.

(Figs. 1a,c). Thus, on average, 19 out of 27 TCs coexisted with UTCLs each year. A total of 345 UTCLs coexisting with TCs were identified, and there were total 593 appearances of UTCLs during active TCs' life spans. This suggests that some of the 251 TCs coexisted with more than one UTCL during their life spans. In fact, we noted the possible influences of six different UTCLs during one TC's life cycle. On the other hand, one UTCL might

appear in several TC events. As far as the possible TC–UTCL interaction is concerned, any TC whose center was located within 15° distance from a UTCL at any time will be included in the sample. There were 153 TCs having interaction with UTCLs, accounting for 61% of the TCs coexisting with UTCLs and 44% of the total TCs. The latter is clearly high enough for operational forecasting consideration of the possible impact of UTCLs on TC activity. In addition, about 97% of the TC–UTCL interaction cases could last for more than 24 h (i.e., at least four events at 6-hourly intervals) continuously. The longest interaction lasts for 150 h, which is about half of the corresponding TC's life span.

Figure 1a shows the annual variation of the numbers of TCs, UTCLs, TCs coexisting with UTCLs, and TCs interacting with UTCLs. No obvious relationship between the UTCL and TC numbers can be seen. In general, the UTCL number exceeded that of the TCs coexisting with UTCLs. The difference between the two numbers was larger after 2002, especially in 2008 with a difference of 16. This may be attributed partly to the improved vertical and horizontal resolutions of the NCEP's Global Forecast System since late October 2002 (http://www.nws.noaa.gov/os/notification/tin02-17gfs.txt). Almost every year the number of TCs coexisting with UTCLs accounted for about 70%–80% of the total TC number, except in 2010 with a percentage of about 90%. However, the number of TCs interacting with UTCLs remained at around 10, except for 2004, in which 19 were noted, and for 2010–12, during which period it increased to 15.

Monthly variation (Fig. 1b) shows that the UTCLs coexisted with TCs only during March–November, although TCs could occur all year-round. The development of TCs coexisting with UTCLs was peaked in August, which is consistent with TC development climatology over WNP (Gray 1968; Chen and Ding 1979) and the UTCL active season (Chen and Chou 1994). Of interest is that the probability of TCs coexisting with UTCLs varied substantially (e.g., from about 90% during the months of June–September to 62% in October and 20% in November). Only one UTCL appeared in both March and April; they formed and then disappeared over the middle ocean (not shown). This feature could be attributed to the absence of active TUTTs in winter, since the TUTT is the major source of UTCLs. The monthly variation of TCs interacting with UTCL is consistent with that of TCs coexisting with UTCLs.

Figure 1c shows that TCs reaching TS and higher intensity categories had higher probabilities to coexist with UTCLs than the TD category, especially for STS with 86% and SuperTY with 83%. The lowest probability for the TD category could be attributed partly to the associated short life spans. Also, the stronger the TC maximum intensity during its life span, the larger probability of the TC interacting with UTCLs, as indicated by an increased percentage from TD (11%) to SuperTY (60%).

Figure 1d presents the number of TCs coexisting with UTCLs and TCs interacting with UTCLs as a function of the time after TC genesis, which reflects the temporal coincidence of UTCLs and TCs. The proportion of the number of TCs coexisting with UTCLs with respect to the total WNP TCs, indicated by black dotted lines, was about 60% after TC genesis. This proportion began to fluctuate after 260 h as the number of longer-lived TCs decreased. For the TCs interacting with UTCLs, both the number and proportion (indicated by red dotted lines) were peaked at 24 h. This can be attributed to some UTCLs that were transformed from an open wave pattern to a closed system during the first 24 h after TC genesis. Then, the proportion decreased to about 10%, at the same rate as the number of the TCs interacting with UTCLs, but it increased for the TCs that lasted for ~190–260 h. While the active periods of TCs overlapped those of UTCLs, it is their relative geographical locations that critically determined the binary vortex interaction between the two systems. This will be examined in the next section.

Figures 2b and 2c show the geographical frequency distribution of the UTCLs that formed as TUTT cells and midlatitude cutoff lows, respectively, in comparison with that of the TCs coexisting with UTCLs given in Fig. 2a. We found that a majority (~83%) of the UTCLs were associated with TUTTs moving westward in tropical easterlies, and only 59 UTCLs were cutoff lows from midlatitude troughs that moved into the target domain; TUTTs and cutoff lows appeared 6815 and 1019 times, respectively, when counted at 6-h intervals (i.e., frequencies shown in Fig. 2). The highest frequency of the TCs coexisting with UTCLs took place over the western portion of WNP and the South China Sea with the mean location at 22.5°N, 131.5°E and the peak location near 18.5°N, 125°E. However, most UTCLs formed from TUTTs appeared over the eastern sector of WNP with the mean location at 22°N, 153°E; they could appear as far south as 5°N and as far west as 100°E in southwestern China. By comparison, cutoff lows from midlatitude westerly troughs were limited to the area to the west of 160°E. A few of them could reach the southern part of the South China Sea from the northwest.

Figure 3 shows the relative positions of TC and UTCL centers at 6-h intervals in order to see their spatial relationship. Several interesting features are worth mentioning. First, we see the dominant zonal distribution of UTCLs that spans from −40° to 70° (west–east) with a south–north width between −30° and 20° relative to the composite TC

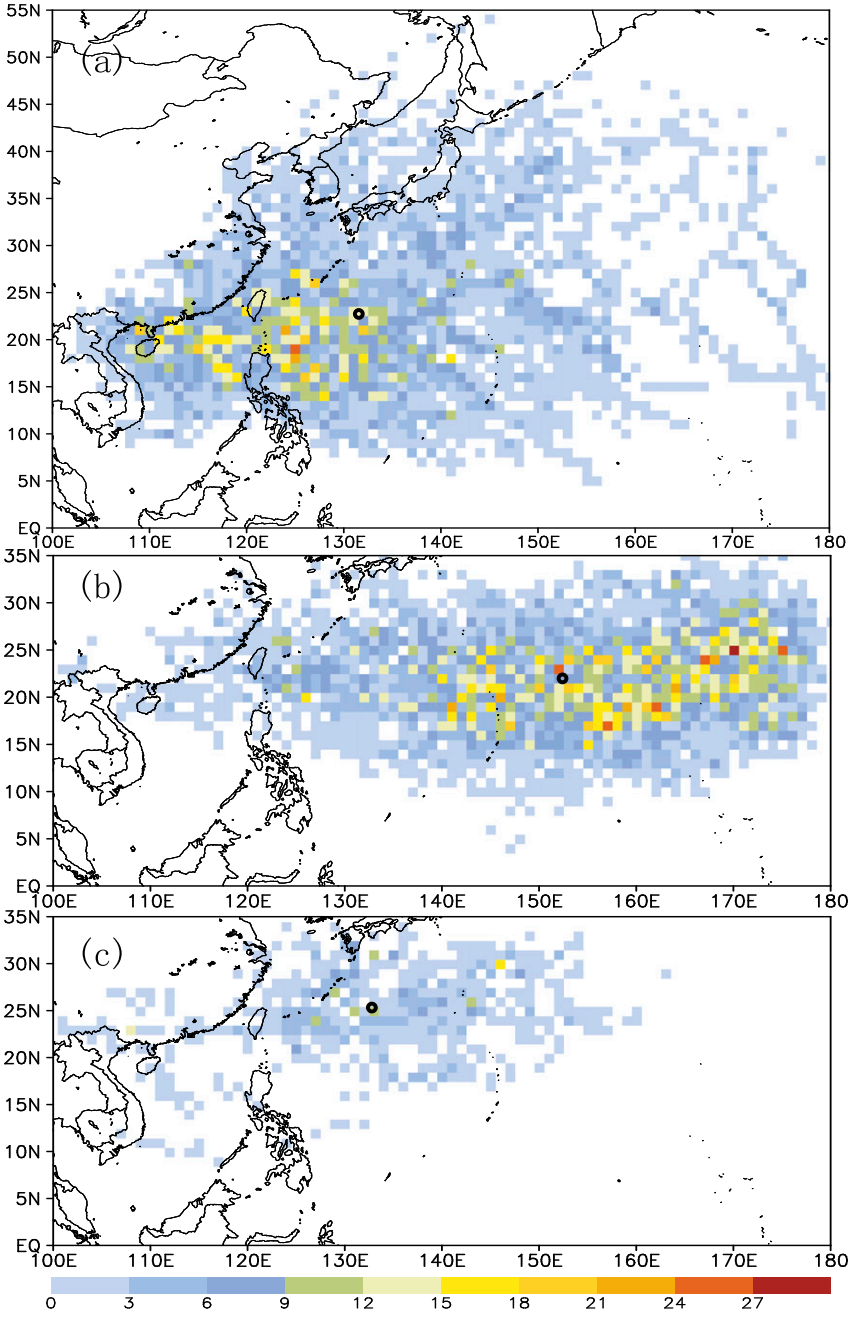

FIG. 2. The geographical frequency distribution of all (a) the TCs coexisting with UTCLs, the UTCLs coexisting with TCs formed from (b) TUTTs and (c) midlatitude cutoff lows over WNP during the years of 2000–12. The frequency is defined as the times of events at 6-h intervals during the period of this study. The shaded boxes denote the 1° × 1° grid resolution of the NCEP FNL data; similarly for the rest of figures. Small black circles in (a)–(c) indicate the mean positions of TCs, TUTTs, and cutoff lows, respectively.

center. Second, most of the UTCLs were located in the east of TCs, because most of them were likely associated with TUTTs in the mid-Pacific. The highest frequency occurred at about 20° to the east of the TC center. In contrast, UTCLs interacting with TCs within a 10° radius distance are more frequently located on the western side of TCs. Only a few coexisting UTCLs took place in the southeastern quadrant of the 10° radius circle.

Third, Fig. 3 reveals the probability of UTCLs coexisting with TCs in different distance ranges during their

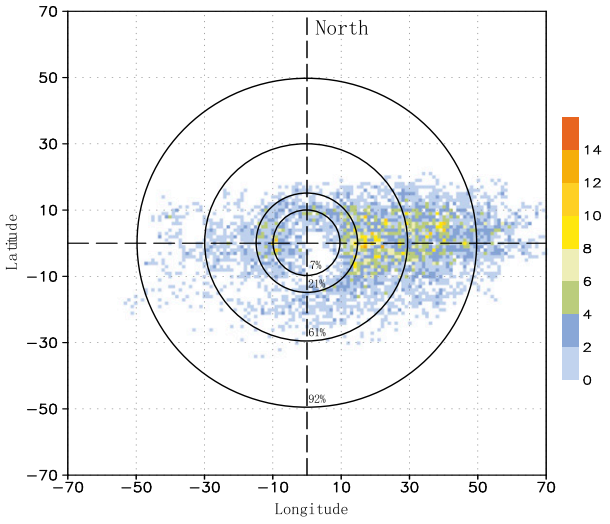

FIG. 3. The spatial frequency distribution of all UTCLs coexisting with TCs relative to the composite TC center over a domain of 140° × 140° longitude–latitude. Quantities inside each circle (i.e., 7% in 10°, 21% in 15°, 61% in 30°, and 92% in 50°) denote the percentages of UTCLs for the covered area with respect to the total UTCLs (see text).

coexisting time periods. Specifically, the overlapping percentage between the two systems increases rapidly from 7% to 92% as the distance between the two systems centers increases from 10° to 50°. As far as the 15° interaction distance is concerned, about 21% of the UTCLs (i.e., a total of 1645 events) were satisfied.

Figure 4 shows the geographical frequency distribution of UTCLs coexisting with TCs within the 15° distance. Apparently, most UTCLs appeared to generate in the eastern sector of WNP (as in Figs. 2b). The higher-frequency UTCL region coincided well with that of active TCs, as indicated by the densely distributed segments of TC tracks (see dotted lines). A comparison of Figs. 4 and 2b,c shows that although only a few UTCLs appeared in China's coastal areas, most of them were within the 15° distance from TC centers, implying the possible impact of UTCLs on the track and intensity changes of landfalling TCs. We have tracked the origins of the UTCLs interacting with TCs, and found that 80% of them were from TUTTs, which is similar to that of the total UTCLs coexisting with TCs.

4. Impact of UTCLs

In this section, a sample, which is made of all the selected cases of TCs and UTCLs interacting at less than 15°, is employed to study the possible impact of UTCL on TC track and intensity change, and the possible impact will be compared to all TCs over WNP within the study period (referred to as the WNP cases or sample hereafter). The WNP climatology is used herein, instead of those TC cases without interaction, to provide a description of the general conditions of TC track and intensity changes over WNP. Given the small percentage

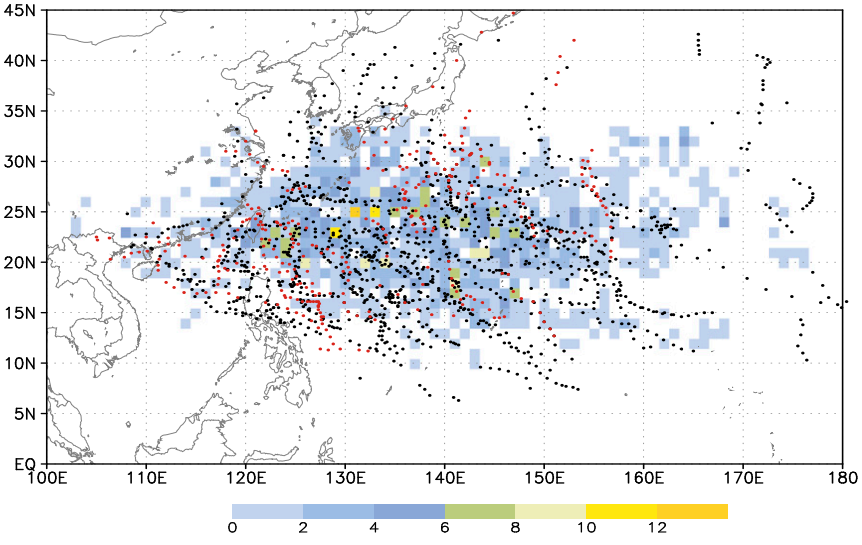

FIG. 4. The geographical frequency distribution over WNP of TCs (dotted) and UTCLs (color shaded) whose respective centers were within a 15° distance. Black dots indicate TCs influenced by TUTT cells, while red dots indicate TCs influenced by cutoff lows from the midlatitudes. Crowded dots accumulated in a grid box imply the passages of more than one TC track at 6-h intervals.

(about 15%) of the TC–UTCL interacting cases with respect to the WNP cases, little differences should be expected when the latter dataset is used.

a. Track changes

To help understand the impact of UTCL on TC track change, we define the direction D of TC movement at a given time T as $D(T)$, with 0° and 90° indicating northward and eastward directions, respectively. Facing the direction of TC movement at time T, the left- and right-turning tracks in the next 6 h (T + 6 h) and 12 h (T + 12 h) are referred to as $D(T + 6/12) - D(T) < 0°$ and $D(T + 6/12) - D(T) > 0°$, respectively, which represent the TC movement tendencies, possibly under the influences of UTCLs. During a 6/12-h period, if $D(T)$ crosses the 0° directional axis from west (east) to east (west), the value of $D(T + 6/12) - D(T)$ will be added (subtracted) to (from) 360°. In addition, if a TC stagnates, the change of $D(T)$ will be 0°. Figure 5 indicates that about 70% of the TCs experienced left and right turnings during their northwestward movements [i.e., $270° < D(T) < 360°$], 20% during their northeastward movements [i.e., $0° < D(T) < 90°$], and only 10% during the southwest and southeastward movements. The proportion of left- and right-turning TCs in the selected sample with respect to those in the WNP sample is also plotted in Fig. 5 (solid lines), showing that TCs with northward movement [i.e., $0° < D(T) < 10°$] had the largest percentage (40%–80%), especially for the left-turning ones. The northwestward (northeastward) moving ones, when interacting with UTCLs, accounted for about 20%–30% (10%–20%) of the total frequency of the WNP cases.

Table 1 shows that the probability of right-turning TCs (50%) at T + 6 h was slightly larger than that of left-turning TCs (47%), with the respective mean directional changes of 15.5° and 14.8°. The probability difference between right- and left-turning TCs increased to 7% at T + 12 h, with the mean directional changes of 22.2° and 20.9°, respectively. However, the higher right-turning tendencies were not significant (at the 95% confidence level). We also see that the frequency of right-turning ones is slightly larger than the left-turning ones when TCs move west-northwestwardly [i.e., $270° < D(T) < 290°$] (Fig. 5). Nevertheless, the mean directional changes of right- and left-turning TCs for the selected cases were slightly smaller than the corresponding TCs for the WNP cases (i.e., 16° and 23° for right turning, and 15.9° and 22.1° for left turning at T + 6 and T + 12 h) (see Table 1). It follows that the impact of UTCL on TC directional change is insignificant when averaged within the 15° interaction distance. This result appears to differ from that obtained by the previous case studies as reviewed in section 1.

Then, we may ask: Will the influence of UTCL on TC directional change depend on their relative distance? To address this question, Fig. 6 shows the frequency and the mean directional changes of the right- and left-turning cases in the selected sample as a function of radius from the composite UTCL center. Like in Fig. 5, the left- and right-turning cases were almost equal in frequency; but their frequencies increased with radius due to the increased area coverage. Of interest is that the left-turning TCs within a 5° radius from the UTCL center experienced greater 6- and 12-h directional changes (i.e., +16.4° and +27.5°) than those (i.e., 15.9° and 22.1°) in the corresponding WNP sample; they are also much larger than 14.8° and 20.9° in the selected sample (Table 1), respectively. In contrast, most left-turning TCs in the 5°–15° radius range made smooth directional changes; similarly for right-turning TCs. A further analysis of the left-turning cases within 5° radius indicates that most of them are associated with weaker storms. That is, TD and TS accounts for about 51% and 44%, respectively, which are much larger than the corresponding 32% and 25%, respectively, of all the left-turning cases within the 15° radius in the WNP climatology.

Next, we examine the azimuthal distribution of the directional changes of TCs relative to the composite UTCL center. The azimuthal distribution is stratified by calculating the mean directional changes with respect to the mean value of the WNP sample (or referred to as the WNP climatology) in eight sectors spanning 45° azimuthally each. It is evident from Fig. 7 that both the right-turning and left-turning TCs in the UTCL's northwestern quadrant experienced negative directional changes (i.e., less directional turning) with respect to the WNP climatology. However, only the right-turning cases in the west-northwestern sector showed a large negative deviation (i.e., −3.4°) with high frequency at T + 6 h to satisfy the significance t test (Fig. 7a). Negative deviations for the left-turning cases also appeared in the west-southwest sector (Figs. 7b,d), but only the cases at T + 12 h (i.e., −4.5°) met the significance t test. Although left-turning cases in the north-northwest sector also present much less directional changes compared to the WNP climatology (i.e., −7.3° at T + 6 h and −9.8° at T + 12 h), due likely to the presence of stronger steering in the midlatitude westerlies, their frequencies were too low to be considered significant (Figs. 7b,d). In contrast, cases in the south-southwestern sector exhibited positive deviations from the WNP climatology at both T + 6 and T + 12 h, especially for the 6-h right-turning ones (i.e., 4.3°) at the 95% confidence level (Fig. 7a). It is found that a majority of TCs in this sector moved northwestward, and their forward speeds tended to be slowed down by the UTCL-induced northwesterly flow.

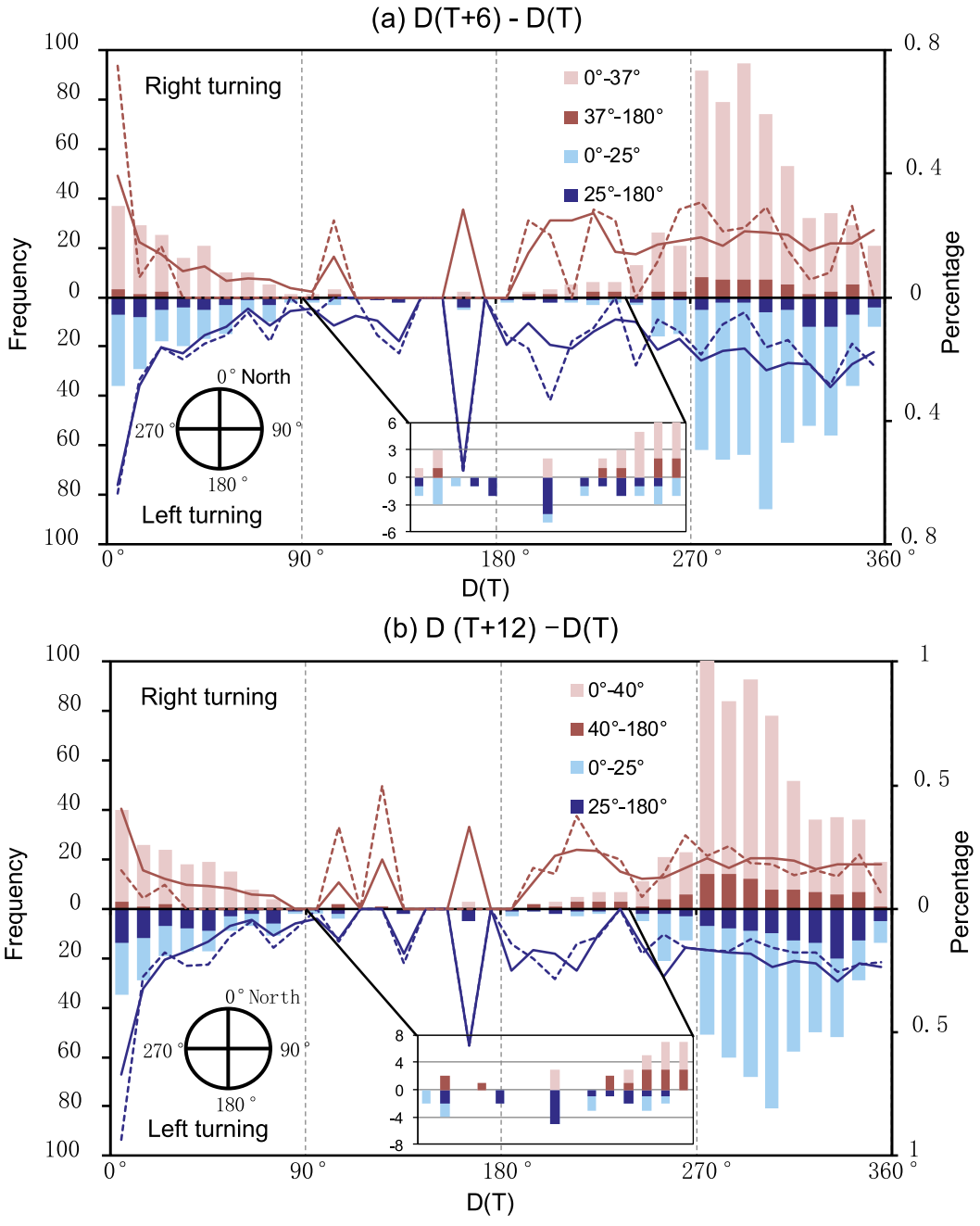

FIG. 5. The frequency distribution of the general directions of TC movement at time T, the right-turning and left-turning directional changes at (a) $T + 6$ and (b) $T + 12$ h, which is stratified by TC tracking direction (every 10°) at time T for the selected cases occurring within a 15° distance. Color scales represent different degrees of directional changes relative to the tracking direction at time T (see the inset notations). The brown (blue) solid line indicates the proportion of right- (left) turning cases in the selected sample with respect to those in the WNP sample. Dashed lines are for abrupt-turning TCs.

Then, the superposition of small, cross-track displacements on the TC velocity are assumed to induce the enhanced directional change. However, the opposing flow of the UTCL seems to affect little on the directional changes of fast-moving TCs in the north-northwest sector. So the directional change depends on the competition of the UTCL-induced steering vectors and TC displacement, and the enhanced turnings are likely to occur when they oppose each other. The TCs in the other sectors did not show significant deviations from

TABLE 1. The percentage (%) and the mean value of directional changes (D in degrees) at $T + 6$ and $T + 12$ h and of intensity changes (I in m s^{-1}) at $T + 12$ and $T + 24$ h relative to their corresponding quantities at $T = 0$ h for the selected sample (i.e., TCs interacting with UTCLs) and the WNP cases. Bold characters denote significant differences at the 95% confidence level compared to the WNP sample.

		All cases		Selected cases	
		Percentage	Mean value	Percentage	Mean value
$D(T + 6) - D(T)$	Right turning	51%	16.0	50%	15.5
	Left turning	43%	15.9	47%	14.8
$D(T + 12) - D(T)$	Right turning	55%	23.0	52%	22.2
	Left turning	41%	22.1	45%	20.9
$I(T + 12) - I(T)$	Intensifying	35%	4.6	47%	4.5
	Weakening	28%	5.4	14%	4.8
$I(T + 24) - I(T)$	Intensifying	46%	7.0	61%	6.9
	Weakening	35%	8.0	17%	6.1

the WNP climatology. Based on the above results, we may state that the impact of UTCLs on TC directional changes is more sensitive to the relative distance than the orientation between the two types of vortices, with more significant interacting radii within about 5°.

For the completeness of this study, it is also of interest to examine to what extent UTCLs would produce any possible impact on the abrupt directional changes of TCs. To this end, we adopt two thresholds of abrupt turnings for the WNP TCs that were developed in a composite study of Wu et al. (2013), which was based on a compromise between the number of available samples, the composite mean value, and the standard derivation of directional changes. That is, an abrupt right turning is defined if a track directional change exceeds 40° (37°) during a 12-h (6 h) period, whereas an abrupt left turning is defined when a track directional change exceeds 25° (25°).

Table 2 shows the percentage of abrupt (left and right) track changes at $T + 6$ h, which accounted for 11.5% of the TCs with directional changes at $T + 6$ h in the selected sample. Abrupt right-turning tracks were mainly associated with TCs moving northwestward [i.e., $270° < D(T) < 320°$], while abrupt left-turning ones occurred when TC movements had a large northward component [i.e., $300° < D(T) < 360°$ and $0° < D(T) < 30°$] (Fig. 5). Although only a few cases moved southwest- and southeastward (see a zoomed view in Fig. 5), 30% of them changed their tracking directions abruptly. The percentage of abrupt right-turning/left-turning TCs interacting with UTCLs with respect to the corresponding WNP climatology stratified by $D(T)$ (dashed lines in Fig. 5) is similar in magnitude and tendency to that of right-turning/left-turning ones (solid lines in Fig. 5). This indicates that few TC experienced abrupt turnings under the influence of UTCLs with respect to the WNP climatology. As compared to the $T + 6$ h track changes, the percentage of total abrupt turning cases at $T + 12$ h almost doubled (i.e., to about 20.2% from 11.5%). Table 2 also shows that the percentage of all abrupt turnings for the WNP and selected samples were similar, indicating that on average UTCLs affect little the abrupt turnings of TCs.

However, the influences of UTCLs on the abrupt turnings of TCs will become notably pronounced when different distances or locations between the two systems are examined. As shown in Fig. 6, the mean directional changes of left-turning cases within a 5° radius reached 32° (i.e., the deviated 16.4° + 15.9° of the WNP climatology) at $T + 6$ h, and 50° (i.e., the deviated 27.5° + 22.1° of the WNP climatology) at $T + 12$ h. They both exceeded the abrupt left-turning criterion of 25°, suggesting that a majority of the left-turning TCs within a distance of 5° from the UTCL center experienced abrupt left turnings. Figures 7b and 7d show that these cases were distributed in the eastern semicircle and south-southwestern sector.

On the other hand, we could see that abrupt turnings of TCs in all quadrants of the UTCL experienced slow displacements. Only a few TCs with more rapid movements in the southeastern and northeastern quadrants had 12-h abrupt right turnings (Fig. 7c), which may be attributed to the abrupt positional changes of TCs from the southern to northern side of subtropical highs. Table 3 shows the mean moving speed for the 6-h and 12-h abrupt turning cases. Of significance is that their mean speeds were 3.7 and 4.2 m s^{-1}, respectively, which were slower than the mean speed of 5.2 m s^{-1} calculated for the selected sample. Similarly, for the WNP sample, we obtained the mean speeds of the 6- and 12-h abrupt track changes as 3.8 and 4.1 m s^{-1}, respectively, which were significantly lower than the climatology of 6.0 m s^{-1}, suggesting that *TCs are likely to slow down during the period of abrupt directional changes.* Figure 7 also shows the asymmetry distribution of TC moving speeds with respect to the UTCL. When TCs entered to the northeastern quadrant of the UTCL, they tended to move northwestward, especially in the east-northeastern sector. This is obvious because TCs over the WNP basin are

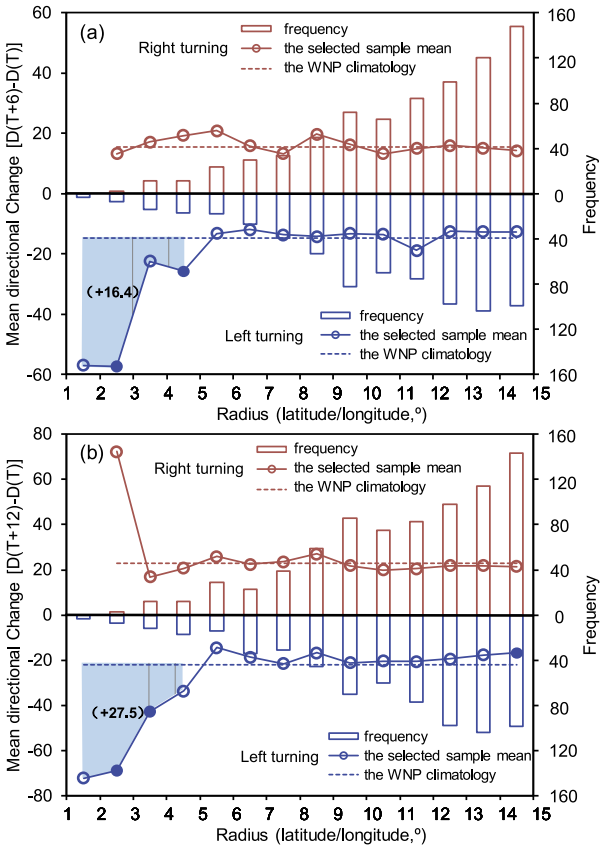

FIG. 6. The frequency (columns) and mean directional change (lines with small circles; unit: °) of TCs in (a) 6 and (b)12 h as a function of distance (in latitude–longitude) from the composite UTCL center for the selected right-turning (brown) and left-turning (blue) cases. Filled circles show significant differences at the 95% confidence level from the corresponding WNP climatology indicated by dashed lines. The quantity with a plus in parentheses shows a significant increase in the mean directional change of the TCs in the shaded distance range over the corresponding WNP climatology.

mainly steered by the easterly or southeasterly flows on the southern side of subtropical highs. In addition, the cyclonic flow of the UTCL, which may extend downward to 700 hPa in the northeastern quadrant (Kelly and Mock 1982), could enhance the steering flow, thus causing faster movements. On the other hand, the UTCL's cyclonic flow could reduce the steering of northwestward-moving TCs in the south-southwestern sector. This is in agreement with the steering effect of UTCLs studied by Chen et al. (2002), which is favorable for the positive deviated directional changes from the WNP climatology (e.g., +4.3° for the right-turning cases shown in Fig. 7a). However, TCs moving into the northwestern quadrant of the UTCL had relatively higher speeds toward the northeast, which was attributable to the presence of strong steering flows ahead of the westerly trough axes in the midlatitudes. These TCs tended to turn right at T + 6 h (cf. Figs. 7a,b) and T + 12 h (cf. Figs. 7c,d) with little directional changes relative to the motion vectors at time T.

We have also analyzed the 24-h directional changes of TCs, and found little statistical significance within 5° radius of the UTCL because of the reduced frequency and likely less influence during 24 h. So they are not shown herein. Other characteristics are similar to those of 6/12-h changes. So we may assume that the UTCL has more significant shorter- than longer-term impact on the track change of TCs, especially their abrupt turnings.

b. *Intensity changes*

To help understand the impact of UTCL on TC intensity change, we define the intensity I of a TC at a given time T, represented by V_{MAX}, as $I(T)$, and then its intensity changes during the following 6, 12, 18, and 24 h are partitioned into an intensifying, maintaining, or weakening category, based on the sign of changes in V_{MAX}. If the sign is positive (negative), a TC event at T is partitioned into the intensifying (weakening) category, and the events with no changes in V_{MAX} are partitioned into the maintaining group. In addition, we ensure that the intensity change of any event, especially over long periods (i.e., 12, 18, and 24 h), must always occur within 15°. With the above partitioning scheme, about 57% of 6-h events in both the selected and WNP samples are categorized into the maintaining group. Such a large percentage of the maintaining events could be attributed to small 6-h intensity changes relative to the 5 m s^{-1} discretization interval that appeared in the CMA/STI's best track data. In fact, the 6-h intensifying and weakening events have an intensity change of 3.4 and −3.9 m s^{-1}, respectively, which are much less than the 5 m s^{-1} discretization interval, as mentioned in section 2. All these imply the presence of little significance of the mean 6-h intensity changes. So, in the next, we will present the results of 12- and 24-h intensity changes as they will be shown to be more than or close to 5 m s^{-1}. The results of 18-h intensity changes will not be shown herein as they are very similar to those of the 24-h intensity changes.

As revealed by Table 1, *intensifying TCs accounted for a large portion of the selected TC cases* (i.e., 47% and 61%, at T + 12 and T + 24 h, respectively), which were significantly larger than the corresponding 35% and 46% of the WNP climatology. However, the mean value of intensity change did not change significantly. In contrast, the percentage of the 12-h weakening cases, when interacting with UTCLs, significantly decreased from 28% to 14%, and of the 24-h weakening ones from 35%

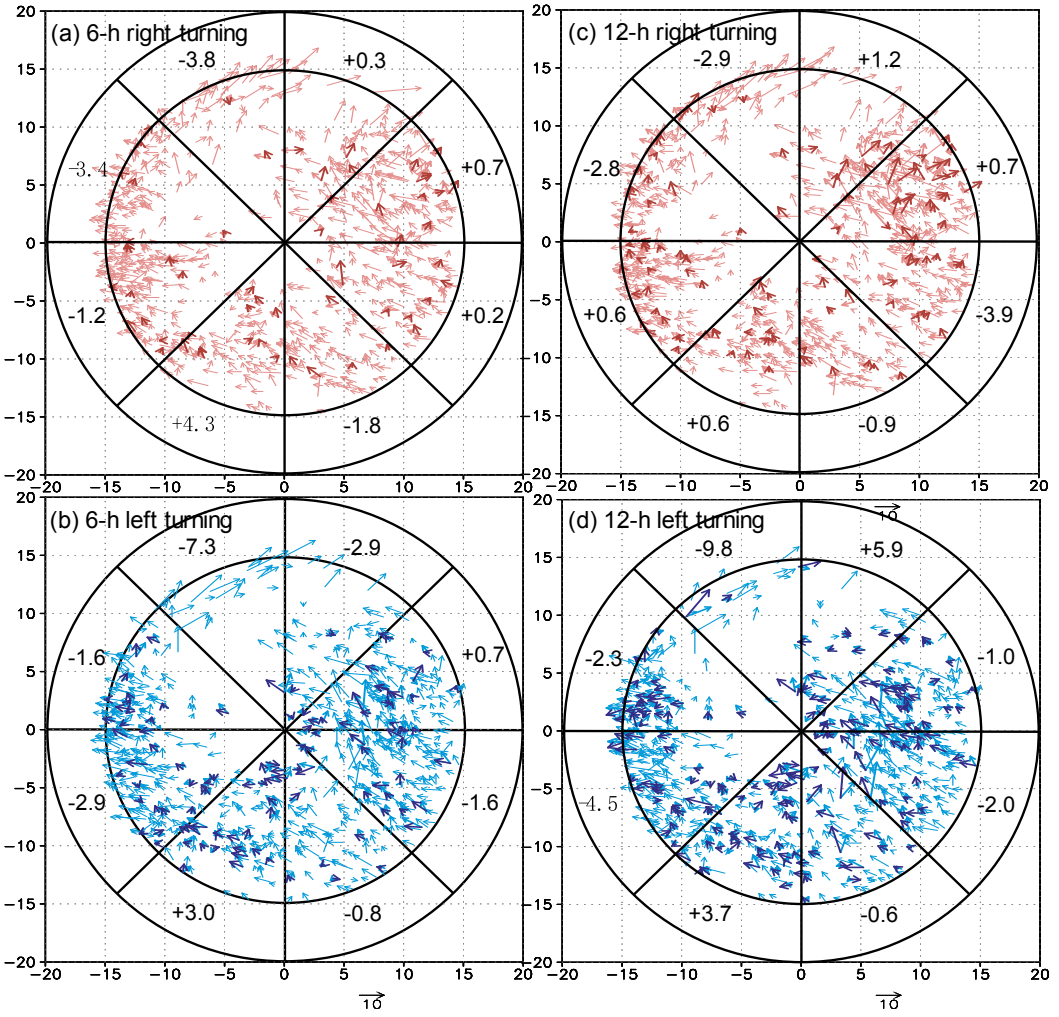

FIG. 7. The spatial distribution of TC motion vectors at time T relative to the composite UTCL center for the selected cases (i.e., TCs interacting with UTCLs) occurring within the interaction distance of 15°: (a) 6-h right-turning, (b) 6-h left-turning, (c) 12-h right-turning, and (d) 12-h left-turning cases. Dark vectors refer to abrupt turning. (bottom) The vector length scale of 10 m s^{-1} is given. The quantity with plus (minus) in the outer circle denotes the increase (decrease) of the 6-h (12 h) mean directional change in each sector compared to the WNP climatology, with the bolded one showing significant differences at the 95% confidence level.

to 17% with a statistically significant decreased mean value (from 8.0 to 6.1 m s^{-1}, i.e., less weakening) compared to the WNP climatology.

A further analysis of these cases indicates that the selected cases were mostly in the TD and TS phases when they were interacting with UTCLs (see Fig. 8), suggesting that a sizeable number of TCs approached UTCLs during their early developing phases. Figure 8 also shows that the frequencies of the intensifying TCs interacting with UTCLs were almost 4 times higher than that of weakening ones during the TD, TS, and STS stages, with the peak frequency at the TD stage. Conversely, intense TCs (i.e., STY and SuperTY stages) might equally become either stronger or weaker when being approached by UTCLs. In general, the percentage of the selected intensifying cases to the corresponding WNP cases decreased with increasing intensity, from about 20% down to almost 0%, as indicated by solid lines in Fig. 8. Note that the average intensity of the selected intensifying cases is significantly weaker than that in all WNP cases (not shown). This suggests that *the impact of UTCLs on intensifying TCs tends to occur during the early development stages of TCs*. However, UTCLs did not have any notable impact on the weakening phases of TCs, as the percentage of the selected weakening cases to the corresponding WNP cases kept at about 5% regardless of TC intensity.

TABLE 2. The percentages (%) of the *abrupt* directional changes (D in degrees) at $T + 6$ and $T + 12$ h, and the *rapid* intensity changes (I in m s^{-1}) at $T + 12$ and $T + 24$ h relative to their corresponding quantities at $T = 0$ h for the selected sample (i.e., TCs interacting with UTCLs) and the WNP sample. Sum denotes the percentage of the total frequency of abrupt or rapid changes to that of the corresponding sample (including maintaining cases).

	Abrupt/rapid changes	All cases	Selected cases
$D(T+6) - D(T)$	Left turning ($\leq -25°$)	17.5%	15.4%
	Right turning ($\geq 37°$)	8.1%	7.9%
	Sum	11.7%	11.5%
$D(T+12) - D(T)$	Left turning ($\leq -25°$)	29.2%	27.0%
	Right turning ($\geq 40°$)	15.0%	14.0%
	Sum	20.2%	20.2%
$I(T+12) - I(T)$	RI (≥ 8 m s^{-1})	11.9%	12.8%
	RW (≤ -9 m s^{-1})	15.3%	8.7%
	Sum	8.4%	7.3%
$I(T+24) - I(T)$	RI (≥ 13 m s^{-1})	10.8%	9.9%
	RW (≤ -15 m s^{-1})	15.6%	8.8%
	Sum	10.4%	7.5%

TABLE 3. The mean speeds (m s^{-1}) of all TC cases and all abrupt (left and right) turning cases in the WNP sample and the selected sample (i.e., TCs interacting with UTCLs).

	All cases	Selected cases
Mean speed	6.0	5.2
Mean speed for 6-h abrupt turning cases	3.8	3.7
Mean speed for 12-h abrupt turning cases	4.1	4.2

Figure 9 shows the frequency and mean intensity changes at $T + 12$ and $T + 24$ h of the intensifying and weakening TCs as a function of radius from the composite UTCL center. We see (i) the presence of a peak frequency in the 9°–10° (13°–14°) radial range for both the $T + 12$ and $T + 24$ h intensifying (weakening) cases; and (ii) similar radial distributions but different amplitudes of intensity changes between the $T + 12$ and $T + 24$ h intensifying cases. Their mean intensity changes within 9° radius, given as bolded quantities in parentheses, were about 15% less than the WNP climatology. Positive deviations from the WNP climatology, albeit small, occurred mainly in the 9°–13° radial range. Significant 12-h intensity changes in the weakening group also occurred in the 9°–13° radial range, with -0.9 m s^{-1} deviation from the WNP climatology (Fig. 9a). Although more pronounced weakening in amplitude was seen in the 3°–6° radial range, it was of small frequency. Significant weakening with high frequencies in the 9°–13° range was also seen for 24-h intensity changes (Fig. 9b). The above results suggest that the effective TC–UTCL interaction radius for intensity changes should be less than 13° rather than 15° as previously used.

Figure 10 shows the spatial frequency distribution of the intensifying and weakening TCs interacting with UTCLs. Obviously, there were more intensifying cases in the southern semicircle (Figs. 10a,c), and more weakening TCs in the west-northwestern and west-southwestern, east-northeastern, and east-southeastern quadrants of the UTCL at both $T + 12$ and $T + 24$ h (Figs. 10b,d). Few intensifying (weakening) cases entered the north-northwestern (south-southeastern) quadrant. These results conform to some extent to the observational study of Kelly and Mock (1982), who indicated more cloudiness in the southern semicircle and dominant subsidence in the northwestern quadrant of a UTCL. Note, though, that the general environment over southern quadrants (e.g., relatively higher SST and weaker VWS) are more favorable than that in northern quadrants for TC intensification, but presumably occurring at a much smaller extent than the influences of UTCLs. The relative amplitudes of deviation in intensity change from the WNP climatology also depend

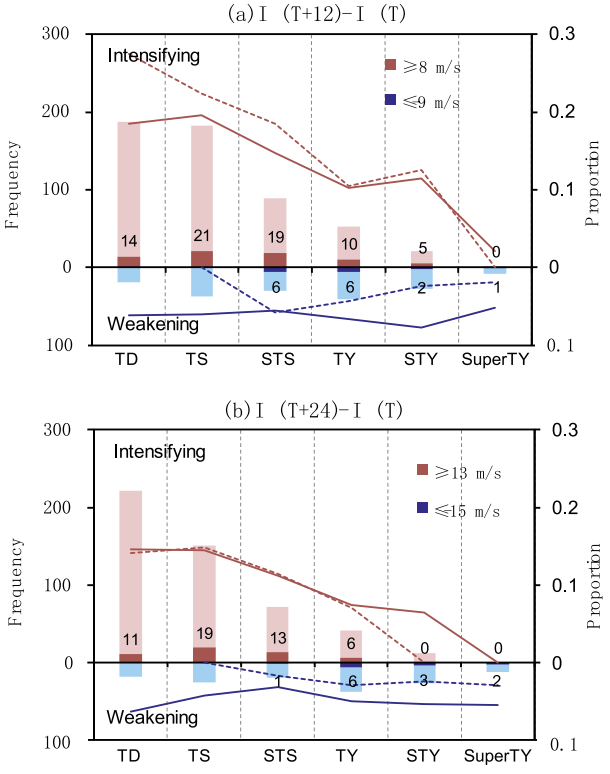

FIG. 8. The frequency (columns) of intensifying and weakening TCs as a function of TC intensity category for the selected cases (i.e., TCs interacting with UTCLs) at (a) $T + 12$ and (b) $T + 24$ h as stratified by TC intensity category at time T. The brown (blue) solid line indicates the proportion of intensifying (weakening) cases in the selected sample to those in the WNP sample. Dashed lines are for RI (RW) cases. Numbers in bars show the frequency of RI/RW in selected sample.

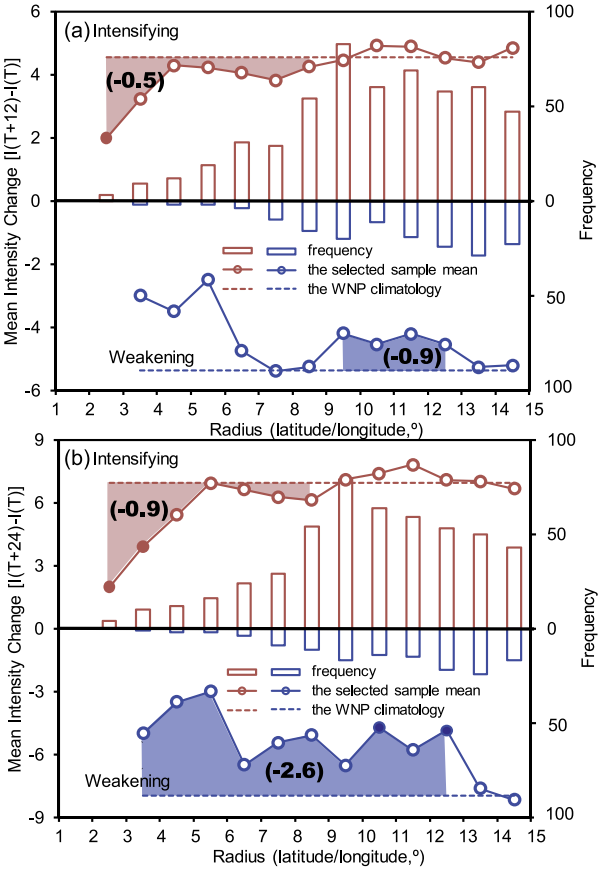

FIG. 9. The frequency (columns) and mean intensity changes (lines with small circles, unit: $m\,s^{-1}$) in (a) 12 and (b) 24 h as a function of radius (in latitude–longitude) from the composite UTCL center for the selected intensifying (brown) and weakening (blue) cases. Filled circles show significant differences at the 95% confidence level from the corresponding WNP climatology (given in Table 1) indicated by dashed lines. The bolded quantity with plus (minus) in parentheses shows a significant increase (decrease) in the mean TC intensity change in the shaded radial range with respect to the corresponding WNP climatology.

on the location of the TC–UTCL interaction. Positive deviations, as indicated by "+," for intensifying cases appeared in most quadrants of the southern semicircle, whereas intensifying TCs in the northern semicircle were negatively influenced. Significant negative deviation from the WNP climatology for 24-h intensifying cases (i.e., $-1.6\,m\,s^{-1}$) occurred in the west-northwestern quadrant. For both 12- and 24-h weakening cases, significant negative deviations occurred in the northeastern quadrants. The reduced weakening from the WNP climatology may be attributed to the presence of some TCs moving northeastward, which are influenced by vertical differential cyclonic vorticity advection ahead of the UTCL. The above results appear to suggest that *TCs in the southern (northern) semicircle of the UTCL are more likely to intensify (weaken), which may represent the "favorable" ("unfavorable") impacts of UTCLs, and that TCs in the UTCL's northeastern quadrant are more likely to weaken slower than those in the WNP climatology.*

Finally, we examine if UTCLs would have any statistically significant impact on the rapid intensity changes of TCs. To our knowledge, a widely accepted definition for rapid intensification (RI) and rapid weakening (RW) in WNP is not available in the literature. But they are definitely accepted as small probability events. Here we define the RI (RW), based on the accumulative percentage approaching to 5% of all the WNP TCs according to Kaplan et al. (2010). An analysis of the WNP cases indicates that we may use 8 (13) $m\,s^{-1}$ as a criterion for RI cases, and -9 (-15) $m\,s^{-1}$ for RW cases during a 12-h (24 h) period. Table 2 shows that the percentages of total RI and RW cases at $T + 12$ h ($T + 24$ h) accounted for 8.4% (RI: 4.2% + RW: 4.2%) and 10.4% (RI: 5% + RW: 5.4%) of the WNP cases, respectively. By comparison, the sum of RI and RW frequencies, when interacting with UTCLs, accounted for 7.3% (7.5%) of the selected sample at $T + 12$ h ($T + 24$ h). Thus, the probability of rapid intensity changes tended to decrease under the influence of UTCLs, more for RW cases (i.e., about 7%). This is due to the fact that most TCs interacting with UTCLs were away from coastal lines where RW is most likely to occur. In contrast, the ±1% differences of RI between the selected and WNP samples imply that on average UTCLs had relatively small influences on the RI of TCs.

Figure 8 shows the intensity categories of TCs when they experience RI or RW. We see that RI tended to occur more frequently during the TS, STS, and TD phases, and decrease at the later stages. The proportion of the selected RI cases to those in the WNP sample, shown by brown-dashed lines in Fig. 8, was similar to that of the intensifying cases. In contrast, there were much fewer RW cases than the RI cases, most of which occurred during the STS and TY phase, whereas few RW cases occurred during TD and TS phases. The distribution of 12-h and 24-h RI cases, shown by black dots in Figs. 10a and 10c, indicates that RI could take place in any sector of the UTCL favoring the intensification of TCs. Notwithstanding, the highest RI frequency appeared in the south-southwestern quadrant, and then the east-southeast quadrant, due likely to the higher mean intensifying rate. It is evident from Figs. 10b and 10d that a majority of RW cases were distributed in the northwest sector of the UTCL. In fact, all of these cases occurred near the coastline of China and Japan, indicating that RW could be attributed mostly to land friction rather than to the influence of UTCLs.

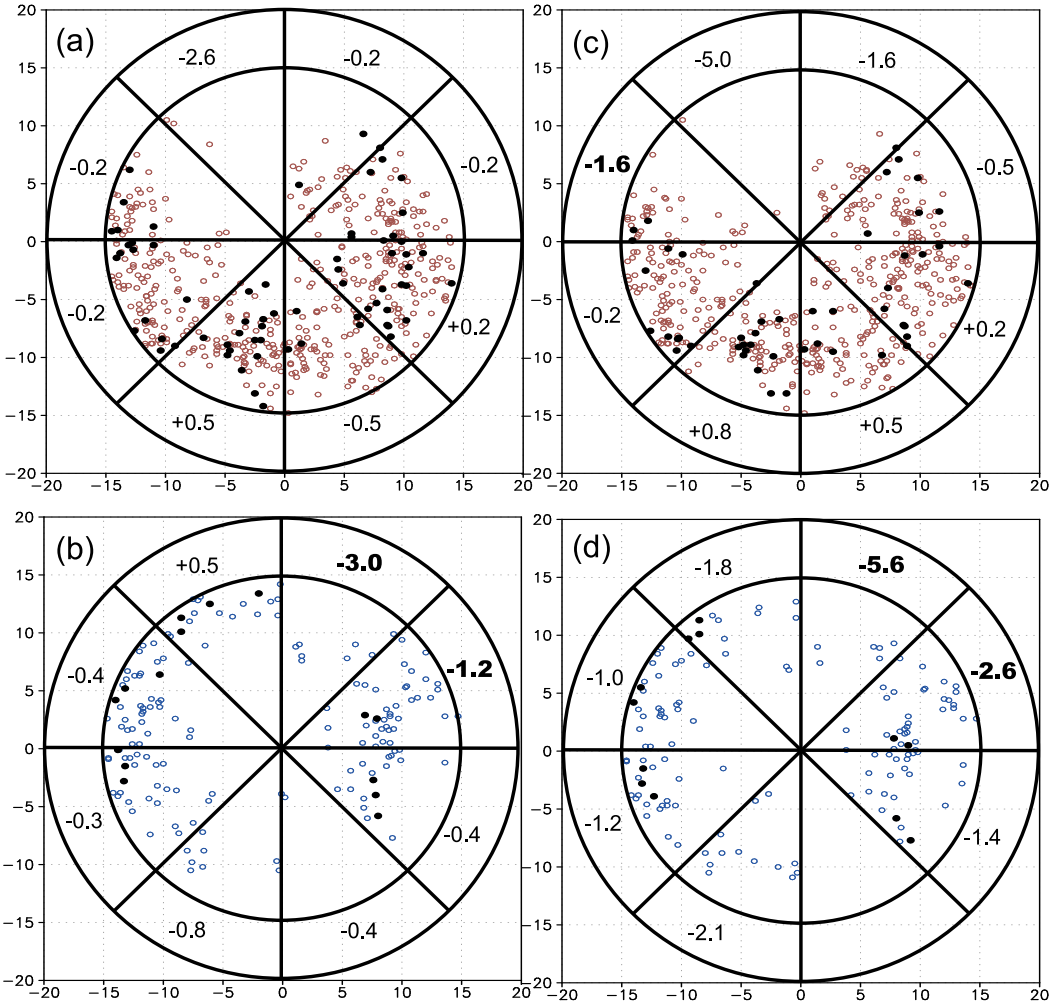

FIG. 10. The spatial frequency distribution of TCs within a 15° distance from the composite UTCL center (with an average location at 23.0°N, 137.4°E) for the selected cases (i.e., TCs interacting with UTCLs) during the subsequent (a) 12-h intensifying, (b) 12-h weakening, (c) 24-h intensifying, and (d) 24-h weakening period. Black dots denote the locations of TCs experiencing rapid intensity changes. The quantity with plus (minus) in the outer circle denotes the enhancement (reduction) of the 12-h (24 h) mean intensity change in each sector over the WNP climatology, with the bolded ones showing significant differences at the 95% confidence level.

5. Summary and conclusions

In this study, the geographical and temporal characteristics of UTCLs and their relationships to the track and intensity changes of WNP TCs occurring during the 13 years of 2000–12 are statistically examined using the CMA-STI best track and the NCEP FNL data. Results show that (i) 83% of the UTCLs originated from TUTTs, and the rest were from cutoff lows in the midlatitude westerlies; (ii) 73% of the WNP TCs coexist with UTCLs, and 90% of them occurred during the months of June–September; and (iii) 44% of the TCs have interaction with UTCLs during their lifetimes, but only 21% of the UTCLs coexisting with TCs were within an interaction distance of 15° due to their different geographical frequency distributions. More UTCLs appeared in the western sectors of TC circulations within a 10° radius.

By selecting those TCs and UTCLs within the 15° interaction distance, on average we find little impact of UTCL on TC directional change, unlike the results obtained by the previous case studies showing the pronounced roles of UTCLs in determining TC track changes. Of course, this finding may not represent the characteristics of some special cases, but highlights the mean characteristics of a large set of cases. Specifically, significant deviations from the 13-yr WNP climatology are found when the azimuthal distribution of TC track changes to a composite UTCL is examined. The right-turning cases in the west-northwestern (south-southwestern) sector at $T + 6$ h showed a large negative

(positive) deviation with high frequency to satisfy the significance t test, and only the left-turning cases in the west-southwestern sector at $T + 12$ h indicated a large negative deviation from the corresponding WNP climatology. A majority of left-turning TCs within a 5° distance experienced abrupt left turnings, albeit with lower frequency, mostly in the eastern semicircle and south-southwestern sector. Moreover, the TC movements tended to be slowed down when undergoing the abrupt directional changes.

Results show that 47%–61% (14%–17%) of the selected TCs intensified (weakened) over 12 and 24 h, which were about 12%–15% higher (lower) than that in the 13-yr WNP climatology, suggesting the statistical significance of UTCLs in TC intensifications, especially during the early development stages. However, it is hard to determine whether the temporal relationship between UTCLs and TC development is causal or merely a correlation. In addition, more intensifying (weakening) TCs were likely to occur in the southern (northern) sectors of UTCLs at both $T + 12$ and $T + 24$ h. Significant less intensification occurred when TCs were located 9° from the composite UTCL center during their intensifying phases, suggesting that the 9° distance between the two systems may be ''unfavorable'' for the further intensification of TCs. In contrast, TCs within the UTCL's 9°–13° radial range, on average, experience little intensification but significantly less weakening during their intensifying and weakening phases, respectively, indicating that more ''favorable'' interaction on TC intensify changes when the centers of the two systems are apart within 9°–13° distance. Results show that RI cases tended to occur in the south-southwestern and east-southeast quadrants of UTCLs, while RW cases appeared in the western semicircle of UTCLs, due mainly to their frequent proximity of mainland coastal regions.

In conclusion, TC track and intensity change could be influenced by UTCL, depending on the sectors of UTCLs in which TCs were positioned, as well as their relative distance. However, it should be noted that although some of the differences in track and intensity changes between the selected cases and the WNP climatology, which are caused by the presence of UTCLs, were relatively small (e.g., less than 5° directional changes or 1 m s^{-1} intensity changes), their significance could not be neglected because of the use of a large sample size. These differences should not be compared to observational uncertainties since the latter represent systematic errors that can be eliminated after taking average. Nevertheless, some cases do show obvious changes when the two systems are located within a certain distance range, such as directional changes up to 90° and intensity changes exceeding 10 m s^{-1}. Of course, TC track and intensity changes involve a chain of many multiscale interactive processes, ranging from the air–sea interaction to easterly waves, large-scale VWS, mesoscale convective systems, cloud microphysics, and the cloud–radiation interaction. Interacting with UTCLs is only one of the processes affecting TC track and intensity changes. Many questions associated with the complicated interactive processes could not be addressed by this and any statistical study. Thus, an in-depth dynamical analysis, which is lacking in our statistical analysis, shall be performed in a future study. Furthermore, the effective interaction could also be affected by the size and intensity of UTCL. More observational and modeling studies are needed to isolate the (positive and negative) impact of UTCLs from other processes, and compare the effects of different sizes and intensities of UTCL on the TC track and intensity change, including their roles in facilitating the abrupt track and rapid intensity changes of TCs.

Acknowledgments. We thank two anonymous reviewers for their constructive comments that have helped significantly improve the quality of this paper. This work was funded by the National Key Basic Research (973) Program of China (Grants 2015CB452804 and 2014CB441402), the Natural Science Foundation of China (Grants 41475055, 91215302, 41175063, and 41275066), and the U.S. Office of Navy Research (Grant N000141410143).

REFERENCES

Bosart, L., W. Bracken, J. Molinari, C. Velden, and P. Black, 2000: Environmental influences on the rapid intensification of Hurricane Opal (1995) over the Gulf of Mexico. *Mon. Wea. Rev.*, **128**, 322–352, doi:10.1175/1520-0493(2000)128<0322:EIOTRI>2.0.CO;2.

Carlson, T., 1967: Structure of a steady-state cold low. *Mon. Wea. Rev.*, **95**, 763–777, doi:10.1175/1520-0493(1967)095<0763:SOASSC>2.3.CO;2.

Chen, G., and L.-F. Chou, 1994: An investigation of cold vortices in the upper troposphere over the western North Pacific during the warm season. *Mon. Wea. Rev.*, **122**, 1436–1448, doi:10.1175/1520-0493(1994)122<1436:AIOCVI>2.0.CO;2.

——, L. Chen, and Y. Lee, 1988: A preliminary study on the western Pacific upper tropospheric cold vortices in the warm months of 1985-1986 (in Chinese). *Meteor. Bull.*, **34**, 275–284.

Chen, L., and Y. Ding, 1979: *An Introduction to the Western Pacific Typhoons* (in Chinese). Science Press, 491 pp.

——, X. Xu, Z. Luo, and J. Wang, 2002: *An Introduction to Tropical Cyclone Dynamics* (in Chinese). Meteorology Press, 317 pp.

Davidson, N., and A. Kumar, 1990: Numerical simulation of the development of AMEX tropical cyclone Irma. *Mon. Wea. Rev.*, **118**, 2001–2019, doi:10.1175/1520-0493(1990)118<2001:NSOTDO>2.0.CO;2.

Davis, C., and L. Bosart, 2004: The TT problem: Forecasting the tropical transition of cyclones. *Bull. Amer. Meteor. Soc.*, **85**, 1657–1662, doi:10.1175/BAMS-85-11-1657.

DeMaria, M., J. Kaplan, and J. Baik, 1993: Upper-level eddy angular momentum fluxes and tropical cyclone intensity change. *J. Atmos. Sci.*, **50**, 1133–1147, doi:10.1175/1520-0469(1993)050<1133:ULEAMF>2.0.CO;2.

Erickson, C., 1971: Diagnostic study of a tropical disturbance. *Mon. Wea. Rev.*, **99**, 67–78, doi:10.1175/1520-0493(1971)099<0067:DSOATD>2.3.CO;2.

Fei, L., and X. Fan, 1992: Numerical simulation and dynamic analysis of influence of upper tropospheric cold vortex on the track of typhoon (in Chinese). *Quart. J. Appl. Meteor.*, **3**, 385–393.

——, and ——, 1993: The influence of structure of upper tropospheric cold vortex on typhoon motion (in Chinese). *Quart. J. Appl. Meteor.*, **4**, 1–7.

Fitzpatrick, P., G. Knaff, C. Landsea, and V. Steven, 1995: Documentation of a systematic bias in the aviation model's forecast of the Atlantic tropical upper-tropospheric trough: Implications for tropical cyclone forecasting. *Wea. Forecasting*, **10**, 433–446, doi:10.1175/1520-0434(1995)010<0433:DOASBI>2.0.CO;2.

Gray, W., 1968: Global view of the origin of tropical disturbances and storms. *Mon. Wea. Rev.*, **96**, 669–700, doi:10.1175/1520-0493(1968)096<0669:GVOTOO>2.0.CO;2.

Hanley, D., 2002: The evolution of a hurricane–trough interaction from a satellite perspective. *Wea. Forecasting*, **17**, 916–926, doi:10.1175/1520-0434(2002)017<0916:TEOAHT>2.0.CO;2.

——, J. Molinari, and D. Keyser, 2001: A composite study of the interactions between tropical cyclones and upper-tropospheric troughs. *Mon. Wea. Rev.*, **129**, 2570–2584, doi:10.1175/1520-0493(2001)129<2570:ACSOTI>2.0.CO;2.

Hart, R., and J. Evans, 1999: Simulations of dual-vortex interaction within environmental shear. *J. Atmos. Sci.*, **56**, 3605–3621, doi:10.1175/1520-0469(1999)056<3605:SODVIW>2.0.CO;2.

Hendricks, E. A., M. T. Montgomery, and C. A. Davis, 2004: The role of vortical hot towers in the formation of Tropical Cyclone Diana (1984). *J. Atmos. Sci.*, **61**, 1209–1232, doi:10.1175/1520-0469(2004)061<1209:TROVHT>2.0.CO;2.

Huo, Z., D.-L. Zhang, and J. Gyakum, 1999: Interaction of potential vorticity anomalies in extratropical cyclogenesis. Part II: Sensitivity to initial perturbations. *Mon. Wea. Rev.*, **127**, 2563–2575, doi:10.1175/1520-0493(1999)127<2563:IOPVAI>2.0.CO;2.

Kaplan, J., M. DeMaria, and A. Knaff, 2010: A revised tropical cyclone rapid intensification index for the Atlantic and eastern North Pacific basins. *Wea. Forecasting*, **25**, 220–241, doi:10.1175/2009WAF2222280.1.

Kelly, W., and D. Mock, 1982: A diagnostic study of upper tropospheric cold lows over the western North Pacific. *Mon. Wea. Rev.*, **110**, 471–480, doi:10.1175/1520-0493(1982)110<0471:ADSOUT>2.0.CO;2.

Kieu, C., and D.-L. Zhang, 2010: A piecewise potential vorticity inversion algorithm and its application to hurricane inner-core anomalies. *J. Atmos. Sci.*, **67**, 2616–2631, doi:10.1175/2010JAS3421.1.

Leroux, M. D., M. Plu, D. Barbary, F. Roux, and P. Arbogast, 2013: Dynamical and physical processes leading to tropical cyclone intensification under upper-level trough forcing. *J. Atmos. Sci.*, **70**, 2547–2565, doi:10.1175/JAS-D-12-0293.1.

Li, Y., L. Guo, Y. Ying, and S. Hu, 2012: Impacts of upper-level cold vortex on the rapid change of intensity and motion of Typhoon Meranti (2010). *J. Trop. Meteor.*, **18**, 207–219.

Miller, B., and T. Carlson, 1970: Vertical motions and the kinetic energy balance of a cold low. *Mon. Wea. Rev.*, **98**, 363–374, doi:10.1175/1520-0493(1970)098<0363:VMATKE>2.3.CO;2.

Molinari, J., and D. Vollaro, 1989: External influences on hurricane intensity. Part I: Outflow layer eddy angular momentum fluxes. *J. Atmos. Sci.*, **46**, 1093–1105, doi:10.1175/1520-0469(1989)046<1093:EIOHIP>2.0.CO;2.

——, S. Skubis, and D. Vollaro, 1995: External influences on hurricane intensity. Part III: Potential vorticity structure. *J. Atmos. Sci.*, **52**, 3593–3606, doi:10.1175/1520-0469(1995)052<3593:EIOHIP>2.0.CO;2.

——, ——, ——, F. Alsheimer, and H. E. Willoughby, 1998: Potential vorticity analysis of tropical cyclone intensification. *J. Atmos. Sci.*, **55**, 2632–2644, doi:10.1175/1520-0469(1998)055<2632:PVAOTC>2.0.CO;2.

Montgomery, M., and B. Farrell, 1993: Tropical cyclone formation. *J. Atmos. Sci.*, **50**, 285–310, doi:10.1175/1520-0469(1993)050<0285:TCF>2.0.CO;2.

——, M. E. Nicholls, T. A. Cram, and A. B. Saunders, 2006: A vortical hot tower route to tropical cyclogenesis. *J. Atmos. Sci.*, **63**, 355–386, doi:10.1175/JAS3604.1.

Palmén, E., 1949: Origin and structure of high-level cyclones south of the maximum westerlies. *Tellus*, **1A**, 22–31, doi:10.1111/j.2153-3490.1949.tb01925.x.

Palmer, C. E., 1953: The impulsive generation of certain changes in the tropospheric circulation. *J. Meteor.*, **10**, 1–9, doi:10.1175/1520-0469(1953)010<0001:TIGOCC>2.0.CO;2.

Patla, J. E., D. Stevens, and G. M. Barnes, 2009: A conceptual model for the influence of TUTT cells on tropical cyclone motion in the Northwest Pacific Ocean. *Wea. Forecasting*, **24**, 1215–1235, doi:10.1175/2009WAF2222181.1.

Persing, J., M. Montgomery, and R. Tuleya, 2002: Environmental interactions in the GFDL Hurricane Model for Hurricane Opal. *Mon. Wea. Rev.*, **130**, 298–317, doi:10.1175/1520-0493(2002)130<0298:EIITGH>2.0.CO;2.

Postel, G. A., and M. H. Hitchman, 1999: A climatology of Rossby wave breaking along the subtropical tropopause. *J. Atmos. Sci.*, **56**, 359–373, doi:10.1175/1520-0469(1999)056<0359:ACORWB>2.0.CO;2.

Rappin, E. D., M. Morgan, and G. Tripoli, 2011: The impact of outflow environment on tropical cyclone intensification and structure. *J. Atmos. Sci.*, **68**, 177–194, doi:10.1175/2009JAS2970.1.

Riehl, H., 1948: On the formation of typhoons. *J. Meteor.*, **5**, 247–265, doi:10.1175/1520-0469(1948)005<0247:OTFOT>2.0.CO;2.

Sadler, J. C., 1976: A role of the tropical upper tropospheric trough in early season typhoon development. *Mon. Wea. Rev.*, **104**, 1266–1278, doi:10.1175/1520-0493(1976)104<1266:AROTTU>2.0.CO;2.

——, 1978: Mid-season typhoon development and intensity changes and the tropical upper tropospheric trough. *Mon. Wea. Rev.*, **106**, 1137–1152, doi:10.1175/1520-0493(1978)106<1137:MSTDAI>2.0.CO;2.

Sears, J., and C. S. Velden, 2014: Investigating the role of the upper levels in tropical cyclogenesis. *Trop. Cyclone Res. Rev.*, **3**, 91–110.

Shi, J.-J., S. W.-J. Chang, and S. Raman, 1990: A numerical study of the outflow layer of tropical cyclones. *Mon. Wea. Rev.*, **118**, 2042–2055, doi:10.1175/1520-0493(1990)118<2042:ANSOTO>2.0.CO;2.

Shieh, H., M. Fiorino, M. Kucas, and B. Wang, 2013: Extreme rapid intensification of Typhoon Vicente (2012) in the South China Sea. *Wea. Forecasting*, **28**, 1578–1587, doi:10.1175/WAF-D-13-00076.1.

Wu, L., P. Ni, J. Duan, and H. Zong, 2013: Sudden tropical cyclone track changes over the western North Pacific: A

composite study. *Mon. Wea. Rev.*, **141**, 2597–2610, doi:10.1175/MWR-D-12-00224.1.

Xu, J., and Y. Wang, 1979: Some synoptic aspects of cold vortexes of tropical upper troposphere over northwest Pacific in summer (in Chinese). *Acta Meteor. Sin.*, **37**, 22–31.

Ying, M., W. Zhang, H. Yu, X. Lu, and J. Feng, 2014: An overview of the China Meteorological Administration tropical cyclone. *J. Atmos. Oceanic Technol.*, **31**, 287–301, doi:10.1175/JTECH-D-12-00119.1.

Zhang, D.-L., and N. Bao, 1996a: Oceanic cyclogenesis as induced by a mesoscale convective system moving offshore. Part I: A 90-h real-data simulation. *Mon. Wea. Rev.*, **124**, 1449–1469, doi:10.1175/1520-0493(1996)124<1449:OCAIBA>2.0.CO;2.

——, and ——, 1996b: Oceanic cyclogenesis as induced by a mesoscale convective system moving offshore. Part II: Genesis and thermodynamic transformation. *Mon. Wea. Rev.*, **124**, 2206–2226, doi:10.1175/1520-0493(1996)124<2206:OCAIBA>2.0.CO;2.